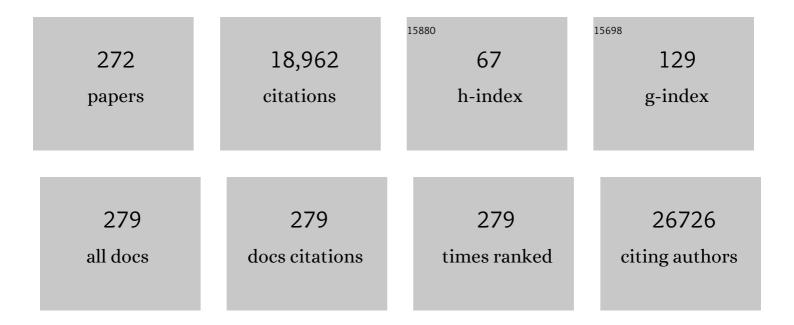
Zheng Xiao Guo

List of Publications by Year in descending order

Source: https://exaly.com/author-pdf/193241/publications.pdf Version: 2024-02-01



ZHENC XIAO CUO

#	Article	IF	CITATIONS
1	Nucleation and growth in solution synthesis of nanostructures – From fundamentals to advanced applications. Progress in Materials Science, 2022, 123, 100821.	16.0	55
2	Indirect to Direct Charge Transfer Transition in Plasmonâ€Enabled CO ₂ Photoreduction. Advanced Science, 2022, 9, e2102978.	5.6	24
3	Negative differential friction coefficients of two-dimensional commensurate contacts dominated by electronic phase transition. Nano Research, 2022, 15, 5758-5766.	5.8	5
4	Effective Ensemble of Pt Single Atoms and Clusters over the (Ni,Co)(OH) ₂ Substrate Catalyzes Highly Selective, Efficient, and Stable Hydrogenation Reactions. ACS Catalysis, 2022, 12, 8104-8115.	5.5	20
5	Co3+-O-V4+ cluster in CoVOx nanorods for efficient and stable electrochemical oxygen evolution. Applied Catalysis B: Environmental, 2021, 282, 119571.	10.8	39
6	TiO2 decorated porous carbonaceous network structures offer confinement, catalysis and thermal conductivity for effective hydrogen storage of LiBH4. Chemical Engineering Journal, 2021, 407, 127156.	6.6	39
7	Multifunctional two-dimensional glassy graphene devices for vis-NIR photodetection and volatile organic compound sensing. Science China Materials, 2021, 64, 1964-1976.	3.5	5
8	Confined Synthesis: From Layered Titanate to Highly Efficient and Durable Mesoporous Cu/TiO ₂ Hydrogen Evolution Photocatalysts. ACS Applied Energy Materials, 2021, 4, 4050-4058.	2.5	8
9	Porosity Engineering of MOFâ€Based Materials for Electrochemical Energy Storage. Advanced Energy Materials, 2021, 11, 2100154.	10.2	75
10	Ferroceneâ€Based Metal–Organic Framework Nanosheets as a Robust Oxygen Evolution Catalyst. Angewandte Chemie - International Edition, 2021, 60, 12770-12774.	7.2	111
11	Ferroceneâ€Based Metal–Organic Framework Nanosheets as a Robust Oxygen Evolution Catalyst. Angewandte Chemie, 2021, 133, 12880-12884.	1.6	4
12	Electrochemical Energy Storage: Porosity Engineering of MOFâ€Based Materials for Electrochemical Energy Storage (Adv. Energy Mater. 20/2021). Advanced Energy Materials, 2021, 11, 2170078.	10.2	4
13	Rational Design of Ptâ^'Pdâ^'Ni Trimetallic Nanocatalysts for Roomâ€Temperature Benzaldehyde and Styrene Hydrogenation. Chemistry - an Asian Journal, 2021, 16, 2298-2306.	1.7	7
14	Developing Nâ€Rich Carbon from C ₃ N ₄ â€Polydopamine Composites for Efficient Oxygen Reduction Reaction. ChemElectroChem, 2021, 8, 3954-3961.	1.7	4
15	Crystallinity-Modulated Co _{2–<i>x</i>} V _{<i>x</i>} O ₄ Nanoplates for Efficient Electrochemical Water Oxidation. ACS Catalysis, 2021, 11, 14884-14891.	5.5	23
16	In Situ Introduction of Li ₃ BO ₃ and NbH Leads to Superior Cyclic Stability and Kinetics of a LiBH ₄ -Based Hydrogen Storage System. ACS Applied Materials & Interfaces, 2020, 12, 893-903.	4.0	21
17	Ambipolar and Robust WSe 2 Fieldâ€Effect Transistors Utilizing Selfâ€Assembled Edge Oxides. Advanced Materials Interfaces, 2020, 7, 1901628.	1.9	11
18	Trace-Level Fluorination of Mesoporous TiO ₂ Improves Photocatalytic and Pb(II) Adsorbent Performances. Inorganic Chemistry, 2020, 59, 17631-17637.	1.9	9

Zheng Xiao Guo

#	Article	IF	CITATIONS
19	A Metal-Free Oxygenated Covalent Triazine 2-D Photocatalyst Works Effectively from the Ultraviolet to Near-Infrared Spectrum for Water Oxidation Apart from Water Reduction. ACS Applied Energy Materials, 2020, 3, 8960-8968.	2.5	7
20	Unique hole-accepting carbon-dots promoting selective carbon dioxide reduction nearly 100% to methanol by pure water. Nature Communications, 2020, 11, 2531.	5.8	168
21	Tuning the interlayer spacing of graphene laminate films for efficient pore utilization towards compact capacitive energy storage. Nature Energy, 2020, 5, 160-168.	19.8	381
22	Assembly of 1T′-MoS ₂ based fibers for flexible energy storage. Nanoscale, 2020, 12, 6562-6570.	2.8	10
23	Stable Complete Water Splitting by Covalent Triazineâ€based Framework CTFâ€0. ChemCatChem, 2020, 12, 2708-2712.	1.8	13
24	Spatially Bandgap-Graded MoS2(1â^'x)Se2x Homojunctions for Self-Powered Visible–Near-Infrared Phototransistors. Nano-Micro Letters, 2020, 12, 26.	14.4	22
25	Ba ₆ In ₆ Zn ₄ Se ₁₉ : a high performance infrared nonlinear optical crystal with [InSe ₃] ^{3â^'} trigonal planar functional motifs. Journal of Materials Chemistry C, 2020, 8, 7947-7955.	2.7	15
26	Flexible and Selfâ€Powered Photodetector Arrays Based on Allâ€Inorganic CsPbBr ₃ Quantum Dots. Advanced Materials, 2020, 32, e2000004.	11.1	134
27	Investigation of metaldehyde removal by powdered activated carbon from different water samples. Environmental Science: Water Research and Technology, 2020, 6, 1432-1444.	1.2	9
28	Strain Engineering of a Defect-Free, Single-Layer MoS ₂ Substrate for Highly Efficient Single-Atom Catalysis of CO Oxidation. ACS Applied Materials & Interfaces, 2019, 11, 32887-32894.	4.0	33
29	Tunable Covalent Triazine-Based Frameworks (CTF-0) for Visible-Light-Driven Hydrogen and Oxygen Generation from Water Splitting. ACS Catalysis, 2019, 9, 7697-7707.	5.5	131
30	Towards rigorous multiscale flow models of nanoparticle reactivity in chemical looping applications. Catalysis Today, 2019, 338, 152-163.	2.2	7
31	The impact of humic acid on metaldehyde adsorption onto powdered activated carbon in aqueous solution. RSC Advances, 2019, 9, 11-22.	1.7	13
32	An efficient carbon-based ORR catalyst from low-temperature etching of ZIF-67 with ultra-small cobalt nanoparticles and high yield. Journal of Materials Chemistry A, 2019, 7, 3544-3551.	5.2	112
33	Synergetic effects of strain engineering and substrate defects on generating highly efficient single-atom catalysts for CO oxidation. Journal of Materials Chemistry A, 2019, 7, 9297-9304.	5.2	12
34	Functionalized Carbon Dots on Graphene as Outstanding Nonâ€Metal Bifunctional Oxygen Electrocatalyst. Small, 2019, 15, e1900296.	5.2	58
35	<i>In situ</i> synthesized low-PtCo@porous carbon catalyst for highly efficient hydrogen evolution. Journal of Materials Chemistry A, 2019, 7, 6543-6551.	5.2	59
36	Enhanced performance of ZnO nanoparticle decorated all-inorganic CsPbBr ₃ quantum dot photodetectors. Journal of Materials Chemistry A, 2019, 7, 6134-6142.	5.2	64

#	Article	IF	CITATIONS
37	Exceptional supercapacitor performance from optimized oxidation of graphene-oxide. Energy Storage Materials, 2019, 17, 12-21.	9.5	135
38	Tunable Bifunctional Activity of Mn x Co3â^'x O4 Nanocrystals Decorated on Carbon Nanotubes for Oxygen Electrocatalysis. ChemSusChem, 2018, 11, 1248-1248.	3.6	5
39	Efficient visible light-driven water oxidation and proton reduction by an ordered covalent triazine-based framework. Energy and Environmental Science, 2018, 11, 1617-1624.	15.6	212
40	High Detectivity and Transparent Fewâ€Layer MoS ₂ /Glassyâ€Graphene Heterostructure Photodetectors. Advanced Materials, 2018, 30, e1706561.	11.1	111
41	Tunable Bifunctional Activity of Mn _{<i>x</i>} Co _{3â^'<i>x</i>} O ₄ Nanocrystals Decorated on Carbon Nanotubes for Oxygen Electrocatalysis. ChemSusChem, 2018, 11, 1295-1304.	3.6	50
42	PbGa ₂ GeS ₆ : An Infrared Nonlinear Optical Material Synthesized by an Intermediate-Temperature Self-Fluxing Method. Crystal Growth and Design, 2018, 18, 1162-1167.	1.4	30
43	Topological phase transitions driven by strain in monolayer tellurium. Physical Review B, 2018, 98, .	1.1	34
44	Cobalt nickel nitride coated by a thin carbon layer anchoring on nitrogen-doped carbon nanotube anodes for high-performance lithium-ion batteries. Journal of Materials Chemistry A, 2018, 6, 19853-19862.	5.2	38
45	Epitaxial Growth of Few‣ayer Black Phosphorene Quantum Dots on Si Substrates. Advanced Materials Interfaces, 2018, 5, 1801048.	1.9	20
46	Solid solution nitride/carbon nanotube hybrids enhance electrocatalysis of oxygen in zinc-air batteries. Energy Storage Materials, 2018, 15, 380-387.	9.5	32
47	Preferential Pt Nanocluster Seeding at Grain Boundary Dislocations in Polycrystalline Monolayer MoS ₂ . ACS Nano, 2018, 12, 5626-5636.	7.3	27
48	Ultrasmall CuCo ₂ S ₄ Nanocrystals: Allâ€inâ€One Theragnosis Nanoplatform with Magnetic Resonance/Nearâ€Infrared Imaging for Efficiently Photothermal Therapy of Tumors. Advanced Functional Materials, 2017, 27, 1606218.	7.8	106
49	From single atoms to self-assembled quantum single-atomic nanowires: noble metal atoms on black phosphorene monolayers. Physical Chemistry Chemical Physics, 2017, 19, 7864-7870.	1.3	1
50	A mechanochemical synthesis of submicron-sized Li ₂ S and a mesoporous Li ₂ S/C hybrid for high performance lithium/sulfur battery cathodes. Journal of Materials Chemistry A, 2017, 5, 6471-6482.	5.2	44
51	Band gap scaling laws in group IV nanotubes. Nanotechnology, 2017, 28, 115202.	1.3	8
52	Amylose-Derived Macrohollow Core and Microporous Shell Carbon Spheres as Sulfur Host for Superior Lithium–Sulfur Battery Cathodes. ACS Applied Materials & Interfaces, 2017, 9, 10717-10729.	4.0	77
53	High efficiency solid-state dye-sensitized solar cells using a cobalt(<scp>ii</scp> / <scp>iii</scp>) redox mediator. Journal of Materials Chemistry C, 2017, 5, 4875-4883.	2.7	14
54	Salt Templating with Pore Padding: Hierarchical Pore Tailoring towards Functionalised Porous Carbons. ChemSusChem, 2017, 10, 199-209.	3.6	24

#	Article	IF	CITATIONS
55	Active sites engineering leads to exceptional ORR and OER bifunctionality in P,N Co-doped graphene frameworks. Energy and Environmental Science, 2017, 10, 1186-1195.	15.6	431
56	A Targeted Functional Design for Highly Efficient and Stable Cathodes for Rechargeable Liâ€lon Batteries. Advanced Functional Materials, 2017, 27, 1604903.	7.8	22
57	Highly crystallized α-FeOOH for a stable and efficient oxygen evolution reaction. Journal of Materials Chemistry A, 2017, 5, 2021-2028.	5.2	140
58	Design of 3D Grapheneâ€Oxide Spheres and Their Derived Hierarchical Porous Structures for High Performance Supercapacitors. Small, 2017, 13, 1702474.	5.2	42
59	An oxidized magnetic Au single atom on doped TiO ₂ (110) becomes a high performance CO oxidation catalyst due to the charge effect. Journal of Materials Chemistry A, 2017, 5, 19316-19322.	5.2	49
60	Multivalency-Driven Formation of Te-Based Monolayer Materials: A Combined First-Principles and Experimental study. Physical Review Letters, 2017, 119, 106101.	2.9	409
61	Self-standing electrodes with core-shell structures for high-performance supercapacitors. Energy Storage Materials, 2017, 9, 119-125.	9.5	52
62	Design of hyperporous graphene networks and their application in solid-amine based carbon capture systems. Journal of Materials Chemistry A, 2017, 5, 17833-17840.	5.2	48
63	Exceptional thermoelectric performance of a "star-like―SnSe nanotube with ultra-low thermal conductivity and a high power factor. Physical Chemistry Chemical Physics, 2017, 19, 23247-23253.	1.3	7
64	Graphitic nanostructures in a porous carbon framework significantly enhance electrocatalytic oxygen evolution. Journal of Materials Chemistry A, 2017, 5, 24686-24694.	5.2	30
65	Nitrogen-Mediated Graphene Oxide Enables Highly Efficient Proton Transfer. Scientific Reports, 2017, 7, 5213.	1.6	4
66	Quasicontinuum simulations of geometric effect on onset plasticity of nano-scale patterned lines. Modelling and Simulation in Materials Science and Engineering, 2017, 25, 065012.	0.8	5
67	Switching effective oxygen reduction and evolution performance by controlled graphitization of a cobalt–nitrogen–carbon framework system. Energy and Environmental Science, 2016, 9, 1661-1667.	15.6	281
68	Relative edge energy in the stability of transition metal nanoclusters of different motifs. Nanoscale, 2016, 8, 12834-12842.	2.8	5
69	Highly Efficient Oxygen Reduction Catalysts by Rational Synthesis of Nanoconfined Maghemite in a Nitrogen-Doped Graphene Framework. ACS Catalysis, 2016, 6, 3558-3568.	5.5	74
70	The effect of Ag, Pb and Bi impurities on grain boundary sliding and intergranular decohesion in Copper. Philosophical Magazine, 2016, 96, 2868-2886.	0.7	9
71	Substrate co-doping modulates electronic metal–support interactions and significantly enhances single-atom catalysis. Nanoscale, 2016, 8, 19256-19262.	2.8	26
72	Interplay between the spin-selection rule and frontier orbital theory in O ₂ activation and CO oxidation by single-atom-sized catalysts on TiO ₂ (110). Physical Chemistry Chemical Physics, 2016, 18, 24872-24879.	1.3	20

#	Article	IF	CITATIONS
73	Anionic Dopants for Improved Optical Absorption and Enhanced Photocatalytic Hydrogen Production in Graphitic Carbon Nitride. Chemistry of Materials, 2016, 28, 7250-7256.	3.2	39
74	Graphene/nitrogen-doped porous carbon sandwiches for the metal-free oxygen reduction reaction: conductivity versus active sites. Journal of Materials Chemistry A, 2016, 4, 12658-12666.	5.2	99
75	Understanding the Hydrophilicity and Water Adsorption Behavior of Nanoporous Nitrogen-Doped Carbons. Journal of Physical Chemistry C, 2016, 120, 18167-18179.	1.5	46
76	Superacidity in Nafion/MOF Hybrid Membranes Retains Water at Low Humidity to Enhance Proton Conduction for Fuel Cells. ACS Applied Materials & Interfaces, 2016, 8, 30687-30691.	4.0	139
77	Naturally Nitrogen and Calcium-Doped Nanoporous Carbon from Pine Cone with Superior CO ₂ Capture Capacities. ACS Sustainable Chemistry and Engineering, 2016, 4, 1050-1057.	3.2	78
78	Highly effective sites and selectivity of nitrogen-doped graphene/CNT catalysts for CO ₂ electrochemical reduction. Chemical Science, 2016, 7, 1268-1275.	3.7	199
79	Highly efficient rutile TiO ₂ photocatalysts with single Cu(<scp>ii</scp>) and Fe(<scp>iii</scp>) surface catalytic sites. Journal of Materials Chemistry A, 2016, 4, 3127-3138.	5.2	73
80	Soy protein directed hydrothermal synthesis of porous carbon aerogels for electrocatalytic oxygen reduction. Carbon, 2016, 96, 622-630.	5.4	84
81	An Ultrahigh Pore Volume Drives Up the Amine Stability and Cyclic CO ₂ Capacity of a Solidâ€Amine@Carbon Sorbent. Advanced Materials, 2015, 27, 4903-4909.	11.1	81
82	Intriguing structures and magic sizes of heavy noble metal nanoclusters around size 55 governed by relativistic effect and covalent bonding. Journal of Chemical Physics, 2015, 143, 174302.	1.2	4
83	Van der Waals Effects on semiconductor clusters. Journal of Computational Chemistry, 2015, 36, 1919-1927.	1.5	5
84	Naturally derived porous carbon with selective metal- and/or nitrogen-doping for efficient CO ₂ capture and oxygen reduction. Journal of Materials Chemistry A, 2015, 3, 5212-5222.	5.2	65
85	Mesoporous Fe ₂ O ₃ flakes of high aspect ratio encased within thin carbon skeleton for superior lithium-ion battery anodes. Journal of Materials Chemistry A, 2015, 3, 14178-14187.	5.2	40
86	A hybrid Si@FeSi _y /SiO _x anode structure for high performance lithium-ion batteries via ammonia-assisted one-pot synthesis. Journal of Materials Chemistry A, 2015, 3, 10767-10776.	5.2	50
87	Carbon Capture: An Ultrahigh Pore Volume Drives Up the Amine Stability and Cyclic CO ₂ Capacity of a Solidâ€Amine@Carbon Sorbent (Adv. Mater. 33/2015). Advanced Materials, 2015, 27, 4902-4902.	11.1	2
88	Visible-light driven heterojunction photocatalysts for water splitting – a critical review. Energy and Environmental Science, 2015, 8, 731-759.	15.6	1,985
89	Compressive Straining of Bilayer Phosphorene Leads to Extraordinary Electron Mobility at a New Conduction Band Edge. Nano Letters, 2015, 15, 2006-2010.	4.5	40
90	Single vacancy defects diffusion at the initial stage of graphene growth: A first-principles study. Physics Letters, Section A: General, Atomic and Solid State Physics, 2015, 379, 1270-1273.	0.9	2

#	Article	IF	CITATIONS
91	Magnetic evolution and anomalous Wilson transition in diagonal phosphorene nanoribbons driven by strain. Nanotechnology, 2015, 26, 295402.	1.3	5
92	Superior CO ₂ adsorption from waste coffee ground derived carbons. RSC Advances, 2015, 5, 29558-29562.	1.7	61
93	Tuning of ZIFâ€Đerived Carbon with High Activity, Nitrogen Functionality, and Yield – A Case for Superior CO ₂ Capture. ChemSusChem, 2015, 8, 2123-2132.	3.6	197
94	Effects of in-plane stiffness and charge transfer on thermal expansion of monolayer transition metal dichalcogenide*. Chinese Physics B, 2015, 24, 026501.	0.7	29
95	An effective template-free synthesis strategy for hierarchical titanium oxide hybrids: tailoring the solvent environment. RSC Advances, 2015, 5, 41059-41065.	1.7	8
96	Sub-surface alloying largely influences graphene nucleation and growth over transition metal substrates. Physical Chemistry Chemical Physics, 2015, 17, 30270-30278.	1.3	4
97	Theoretical study of hydration in Y2Mo3O12: Effects on structure and negative thermal expansion. AIP Advances, 2015, 5, .	0.6	17
98	Effect of Nitrogen Doping on the CO ₂ Adsorption Behavior in Nanoporous Carbon Structures: A Molecular Simulation Study. Journal of Physical Chemistry C, 2015, 119, 22310-22321.	1.5	108
99	Graphene-based materials: Synthesis and gas sorption, storage and separation. Progress in Materials Science, 2015, 69, 1-60.	16.0	601
100	Intrinsic spin dependent and ferromagnetic stability on edge saturated zigzag graphene-like carbon-nitride nanoribbons. Applied Physics Letters, 2014, 104, 172111.	1.5	8
101	Highâ€Performance All arbon Yarn Microâ€Supercapacitor for an Integrated Energy System. Advanced Materials, 2014, 26, 4100-4106.	11.1	223
102	Flexible and Binderâ€Free Organic Cathode for Highâ€Performance Lithiumâ€Ion Batteries. Advanced Materials, 2014, 26, 3338-3343.	11.1	200
103	Hierarchically porous graphene sheets and graphitic carbon nitride intercalated composites for enhanced oxygen reduction reaction. Journal of Materials Chemistry A, 2014, 2, 3209-3215.	5.2	61
104	Postsynthesis Annealing of MOF-5 Remarkably Enhances the Framework Structural Stability and CO ₂ Uptake. Chemistry of Materials, 2014, 26, 6333-6338.	3.2	126
105	Highly Efficient Photocatalytic H ₂ Evolution from Water using Visible Light and Structure ontrolled Graphitic Carbon Nitride. Angewandte Chemie - International Edition, 2014, 53, 9240-9245.	7.2	1,000
106	Nitrogen-enriched and hierarchically porous carbon macro-spheres – ideal for large-scale CO ₂ capture. Journal of Materials Chemistry A, 2014, 2, 5481-5489.	5.2	66
107	Exceptional CO ₂ capture in a hierarchically porous carbon with simultaneous high surface area and pore volume. Energy and Environmental Science, 2014, 7, 335-342.	15.6	385
108	Selective morphologies of MgO via nanoconfinement on γ-Al ₂ O ₃ and reduced graphite oxide (rGO): improved CO ₂ capture capacity at elevated temperatures. CrystEngComm, 2014, 16, 8825-8831.	1.3	9

#	Article	IF	CITATIONS
109	Atomistic view of thin Ni/Ni3Al (0 0 1) under uniaxial tension of twist grain boundaries. RSC Advances, 2014, 4, 4552-4557.	1.7	12
110	Enhanced hydrogen desorption of an ammonia borane and lithium hydride system through synthesised intermediate compounds. Journal of Materials Chemistry A, 2014, 2, 6801-6813.	5.2	6
111	Role of Charge Transfer in Dehydrogenation of M(NH ₂ BH ₃) ₂ (M =) Tj ETC	2q1_1 0.78	34314 rgBT /(
112	Negative thermal expansion in TiF3 from the first-principles prediction. Physics Letters, Section A: General, Atomic and Solid State Physics, 2014, 378, 2906-2909.	0.9	14
113	First-principles investigation of negative thermal expansion in II-VI semiconductors. Materials Chemistry and Physics, 2014, 148, 214-222.	2.0	23
114	Strain and Orientation Modulated Bandgaps and Effective Masses of Phosphorene Nanoribbons. Nano Letters, 2014, 14, 4607-4614.	4.5	306
115	A thermally derived and optimized structure from ZIF-8 with giant enhancement in CO ₂ uptake. Energy and Environmental Science, 2014, 7, 2232-2238.	15.6	222
116	Fe ₂ O ₃ –TiO ₂ Nanocomposites for Enhanced Charge Separation and Photocatalytic Activity. Chemistry - A European Journal, 2014, 20, 15571-15579.	1.7	146
117	First-principles study of tetragonal PbTiO3: Phonon and thermal expansion. Materials Research Bulletin, 2014, 49, 509-513.	2.7	28
118	Overview on Hydrogen Absorbing Materials. Advances in Chemical and Materials Engineering Book Series, 2014, , 312-342.	0.2	0
119	Dehydrogenation mechanisms of Ca(NH2BH3)2: TheÂless the charge transfer, the lower the barrier. International Journal of Hydrogen Energy, 2013, 38, 11313-11320.	3.8	8
120	Structural and reaction pathway analyses of Mg(BH4)2·2NH3 for hydrogen storage : A first-principles study. International Journal of Hydrogen Energy, 2013, 38, 2836-2845.	3.8	7
121	Ca(BH4)2–LiBH4–MgH2: a novel ternary hydrogen storage system with superior long-term cycling performance. Journal of Materials Chemistry A, 2013, 1, 12285.	5.2	35
122	Improved hydrogen storage performance of Ca(BH4)2: a synergetic effect of porous morphology and in situ formed TiO2. Energy and Environmental Science, 2013, 6, 847.	15.6	35
123	First-principles study of stacking fault energies in Mg-based binary alloys. Computational Materials Science, 2013, 79, 564-569.	1.4	107
124	Static recrystallization and grain growth during annealing of an extruded Mg–Zn–Zr–Er magnesium alloy. Journal of Magnesium and Alloys, 2013, 1, 31-38.	5.5	46
125	Negative thermal expansion correlated with polyhedral movements and distortions in orthorhombic Y2Mo3O12. Materials Research Bulletin, 2013, 48, 2724-2729.	2.7	60
126	Nanoconfined ammonia borane in a flexible metal–organic framework Fe–MIL-53: clean hydrogen release with fast kinetics. Journal of Materials Chemistry A, 2013, 1, 4167.	5.2	66

#	Article	IF	CITATIONS
127	Tin clusters formed by fundamental units: a potential way to assemble tin nanowires. Physical Chemistry Chemical Physics, 2013, 15, 1831-1836.	1.3	14
128	MgH ₂ Dehydrogenation Thermodynamics: Nanostructuring and Transition Metal Doping. Journal of Physical Chemistry C, 2013, 117, 10883-10891.	1.5	62
129	Novel methods to fabricate macroporous 3D carbon scaffolds and ordered surface mesopores on carbon filaments. Journal of Porous Materials, 2012, 19, 529-536.	1.3	7
130	Structure and Defect Chemistry of Low- and High-Temperature Phases of LiBH ₄ . Journal of Physical Chemistry C, 2012, 116, 13488-13496.	1.5	25
131	Threadlike Tin Clusters with High Thermal Stability Based on Fundamental Units. Journal of Physical Chemistry C, 2012, 116, 231-236.	1.5	8
132	Multi-hydride systems with enhanced hydrogen storage properties derived from Mg(BH4)2 and LiAlH4. International Journal of Hydrogen Energy, 2012, 37, 10733-10742.	3.8	48
133	Materials challenges for the development of solid sorbents for post-combustion carbon capture. Journal of Materials Chemistry, 2012, 22, 2815-2823.	6.7	255
134	Porous anodes with helical flow pathways in bioelectrochemical systems: The effects of fluid dynamics and operating regimes. Journal of Power Sources, 2012, 213, 382-390.	4.0	49
135	Structural, energetic and thermodynamic analyses of Ca(BH4)2·2NH3 from first principles calculations. Journal of Solid State Chemistry, 2012, 185, 206-212.	1.4	10
136	High inertness of W@Si12 cluster toward O2 molecule. Physics Letters, Section A: General, Atomic and Solid State Physics, 2012, 376, 1454-1459.	0.9	6
137	Calcium-Based Functionalization of Carbon Materials for CO ₂ Capture: A First-Principles Computational Study. Journal of Physical Chemistry C, 2011, 115, 10990-10995.	1.5	51
138	Dehydrogenation mechanisms and thermodynamics of MNH2BH3 (M = Li, Na) metal amidoboranes as predicted from first principles. Physical Chemistry Chemical Physics, 2011, 13, 7649.	1.3	41
139	Processing of strong and highly conductive carbon foams as electrode. Carbon, 2011, 49, 3857-3864.	5.4	51
140	Effect of nitride additives on Li–N–H hydrogen storage system. International Journal of Hydrogen Energy, 2011, 36, 7920-7926.	3.8	24
141	First-principles calculations on the role of Ni-doping in Cu clusters: From geometric and electronic structures to chemical activities towards CO2. Physics Letters, Section A: General, Atomic and Solid State Physics, 2010, 374, 4324-4330.	0.9	24
142	Partition of Er among the constituent phases and the yield phenomenon in a semi-continuously cast Mg–Zn–Zr alloy. Scripta Materialia, 2010, 63, 367-370.	2.6	38
143	Site density effect of Ni particles on hydrogen desorption of MgH2. International Journal of Hydrogen Energy, 2010, 35, 4534-4542.	3.8	46
144	First-principles study of the stability of calcium-decorated carbon nanostructures. Physical Review B, 2010. 82	1.1	53

#	Article	IF	CITATIONS
145	CO ₂ Activation and Total Reduction on Titanium(0001) Surface. Journal of Physical Chemistry C, 2010, 114, 11456-11459.	1.5	34
146	Multinuclear Zinc Pentafluorobenzene Carboxylates: Synthesis, Characterization, and Hydrogen Storage Capability. Organometallics, 2010, 29, 6129-6132.	1.1	24
147	Advances in computational studies of energy materials. Philosophical Transactions Series A, Mathematical, Physical, and Engineering Sciences, 2010, 368, 3379-3456.	1.6	119
148	Enhancement of H2 uptake via fluorination but not lithiation for Zn4N8 and Zn4N6O type clusters. Chemical Communications, 2010, 46, 9055.	2.2	11
149	hcp metal nanoclusters with hexagonalAâ^'Abilayer stacking stabilized by enhanced covalent bonding. Physical Review B, 2010, 82, .	1.1	15
150	Role of Ag-doping in small transition metal clusters from first-principles simulations. Journal of Chemical Physics, 2009, 131, 184301.	1.2	13
151	Synthesis of a porous oxide layer on a multifunctional biomedical titanium by micro-arc oxidation. Materials Science and Engineering C, 2009, 29, 1923-1934.	3.8	47
152	Microstructure and mechanical properties of a spark plasma sinteredTi–45Al–8.5Nb–0.2W–0.2B–0.1Y alloy. Intermetallics, 2009, 17, 840-846.	1.8	52
153	High-temperature oxidation behavior of TiAl-based alloys fabricated by spark plasma sintering. Journal of Alloys and Compounds, 2009, 478, 220-225.	2.8	33
154	Density functional theory simulations of complex hydride and carbon-based hydrogen storage materials. Chemical Society Reviews, 2009, 38, 211-225.	18.7	107
155	Hydrogen Absorption/Desorption Mechanism in Potassium Alanate (KAlH ₄) and Enhancement by TiCl ₃ Doping. Journal of Physical Chemistry C, 2009, 113, 6845-6851.	1.5	48
156	The Formation of Nanocrystallite Bone-Like Apatite on Chemically Treated Ti-24Nd-4Zr-7.9Sn Alloy. Journal of Nanoscience and Nanotechnology, 2009, 9, 1214-1217.	0.9	2
157	Fabrication of porous titanium scaffold materials by a fugitive filler method. Journal of Materials Science: Materials in Medicine, 2008, 19, 3489-3495.	1.7	29
158	Materials challenges for hydrogen storage. Journal of the European Ceramic Society, 2008, 28, 1467-1473.	2.8	48
159	Effects of different carbon materials on MgH2 decomposition. Carbon, 2008, 46, 126-137.	5.4	158
160	Multiscale simulation of onset plasticity during nanoindentation of Al (001) surface. Acta Materialia, 2008, 56, 4358-4368.	3.8	57
161	Effect of milling conditions on structural evolution and phase stability of [Ti(H2)+Al+Nb] powder mixtures. Materials Science & Engineering A: Structural Materials: Properties, Microstructure and Processing, 2008, 474, 173-180.	2.6	12
162	High-Capacity Room-Temperature Hydrogen Storage in Carbon Nanotubes via Defect-Modulated Titanium Doping. Journal of Physical Chemistry C, 2008, 112, 17456-17464.	1.5	71

#	Article	IF	CITATIONS
163	Effects of Carbon-Supported Nickel Catalysts on MgH2Decomposition. Journal of Physical Chemistry C, 2008, 112, 5984-5992.	1.5	62
164	No Cage, No Tube: Relative Stabilities of Nanostructures. Journal of Physical Chemistry C, 2008, 112, 13200-13203.	1.5	11
165	Oxidation investigation of nickel nanoparticles. Physical Chemistry Chemical Physics, 2008, 10, 5057.	1.3	110
166	Structure, optical properties and defects in nitride (Ill–V) nanoscale cage clusters. Physical Chemistry Chemical Physics, 2008, 10, 1944.	1.3	42
167	Multiple-Timescale Photoreactivity of a Model Compound Related to the Active Site of [FeFe]-Hydrogenase. Inorganic Chemistry, 2008, 47, 7453-7455.	1.9	41
168	Size- and charge-dependent geometric and electronic structures of Binâ€^(Binâ^') clusters (n=2–13) by first-principles simulations. Journal of Chemical Physics, 2008, 128, 194304.	1.2	34
169	First-principles local density approximation (generalized gradient approximation) +U study of catalytic CenOm clusters: U value differs from bulk. Journal of Chemical Physics, 2008, 128, 164718.	1.2	21
170	Hydrogen-induced magnetization and tunable hydrogen storage in graphitic structures. Physical Review B, 2008, 77, .	1.1	33
171	Effect of ultrasound on the heterogeneous nucleation of BaSO4 during reactive crystallization. Journal of Applied Physics, 2007, 101, 054907.	1.1	18
172	Initial interactions between water molecules and Ti-adsorbed carbon nanotubes. Applied Physics Letters, 2007, 91, 161906.	1.5	11
173	Coupled mesoscopic constitutive modelling and finite element simulation for plastic flow and microstructure of two-phase alloys. Computational Materials Science, 2007, 40, 201-212.	1.4	4
174	Desorption characteristics of mechanically and chemically modified LiNH2 and (LiNH2+LiH). Journal of Alloys and Compounds, 2007, 432, 277-282.	2.8	60
175	Effect of composition on the microstructure and mechanical properties of Mg–Zn–Al alloys. Materials Science & Engineering A: Structural Materials: Properties, Microstructure and Processing, 2007, 456, 43-51.	2.6	104
176	Hydrogen sorption in defective hexagonal BN sheets and BN nanotubes. Physical Review B, 2007, 76, .	1.1	128
177	Reaction Paths between LiNH2 and LiH with Effects of Nitrides. Journal of Physical Chemistry B, 2007, 111, 12531-12536.	1.2	54
178	Structural and desorption characterisations of milled (MgH2+Y,Ce)(MgH2+Y,Ce) powder mixtures for hydrogen storage. International Journal of Hydrogen Energy, 2007, 32, 2920-2925.	3.8	45
179	High-speed observation of the effects of ultrasound on liquid mixing and agglomerated crystal breakage processes. Powder Technology, 2007, 171, 146-153.	2.1	46
180	Electronic structure, stability and bonding of the Li-N-H hydrogen storage system. Physical Review B, 2006, 74, .	1.1	68

#	Article	IF	CITATIONS
181	Transition-metal-doping-enhanced hydrogen storage in boron nitride systems. Applied Physics Letters, 2006, 89, 153104.	1.5	75
182	Solidification microstructural constituent and its crystallographic morphology of permanent-mould-cast Mg-Zn-Al alloys. Transactions of Nonferrous Metals Society of China, 2006, 16, 452-458.	1.7	26
183	A First-Principles Study of the Electronic Structure and Stability of a Lithium Aluminum Hydride for Hydrogen Storage. Journal of Physical Chemistry B, 2006, 110, 6906-6910.	1.2	22
184	Experimental and molecular dynamics studies of the thermal decomposition of a polyisobutylene binder. Acta Materialia, 2006, 54, 4803-4813.	3.8	8
185	display="inline" overflow="scroll" xmlns:xocs="http://www.elsevier.com/xml/xocs/dtd" xmlns:xs="http://www.w3.org/2001/XMLSchema" xmlns:xsi="http://www.w3.org/2001/XMLSchema-instance" xmlns="http://www.elsevier.com/xml/ja/dtd" xmlns:ja="http://www.elsevier.com/xml/ja/dtd" xmlns:mml="http://www.w3.org/1998/Math/MathML"	1.9	79
186	Interpretation of the ultrasonic effect on induction time during BaSO4 homogeneous nucleation by a cluster coagulation model. Journal of Colloid and Interface Science, 2006, 297, 190-198.	5.0	27
187	Metastable MgH2 phase predicted by first principles calculations. Applied Physics Letters, 2006, 89, 111911.	1.5	14
188	Effect of ultrasound on anti-solvent crystallization process. Journal of Crystal Growth, 2005, 273, 555-563.	0.7	194
189	Phase transformation during aging and resulting mechanical properties of two Ti–Nb–Ta–Zr alloys. Materials Science and Technology, 2005, 21, 678-686.	0.8	20
190	Influence of selected alloying elements on the stability of magnesium dihydride for hydrogen storage applications: A first-principles investigation. Physical Review B, 2004, 69, .	1.1	185
191	Numerical heat transfer modelling for wire casting. Materials Science & Engineering A: Structural Materials: Properties, Microstructure and Processing, 2004, 365, 311-317.	2.6	18
192	Mechanical alloying and electronic simulations of (MgH2+M) systems (M=Al, Ti, Fe, Ni, Cu and Nb) for hydrogen storage. International Journal of Hydrogen Energy, 2004, 29, 73-80.	3.8	376
193	Influence of titanium on the hydrogen storage characteristics of magnesium hydride: a first principles investigation. Materials Science & Engineering A: Structural Materials: Properties, Microstructure and Processing, 2004, 365, 73-79.	2.6	48
194	Kinetic modelling of binder removal in powder-based compacts. Materials Science & Engineering A: Structural Materials: Properties, Microstructure and Processing, 2004, 365, 129-135.	2.6	4
195	Microstructural evolution of a Ti–6Al–4V alloy during β-phase processing: experimental and simulative investigations. Materials Science & Engineering A: Structural Materials: Properties, Microstructure and Processing, 2004, 365, 172-179.	2.6	157
196	Cellular automata simulation of microstructural evolution during dynamic recrystallization of an HY-100 steel. Materials Science & Engineering A: Structural Materials: Properties, Microstructure and Processing, 2004, 365, 180-185.	2.6	95
197	A 3D conjugate heat transfer model for continuous wire casting. Materials Science & Engineering A: Structural Materials: Properties, Microstructure and Processing, 2004, 365, 318-324.	2.6	18
198	Fluid dynamic simulations of a slurry coating process on a continuous fibre. Materials Science & Engineering A: Structural Materials: Properties, Microstructure and Processing, 2004, 365, 341-348.	2.6	4

#	Article	IF	CITATIONS
199	Wear characteristics of Ti–Nb–Ta–Zr and Ti–6Al–4V alloys for biomedical applications. Wear, 2004, 257, 869-876.	1.5	138
200	Study of thermal decomposition of a polyisobutylene binder by molecular dynamic simulations. Materials Science & Engineering A: Structural Materials: Properties, Microstructure and Processing, 2004, 365, 122-128.	2.6	3
201	Artificial neural network modelling of hydrogen storage properties of Mg-based alloys. Materials Science & Engineering A: Structural Materials: Properties, Microstructure and Processing, 2004, 365, 219-227.	2.6	38
202	Finite element modelling of composite consolidation from fibre and wire lay-ups. Materials Science & Engineering A: Structural Materials: Properties, Microstructure and Processing, 2004, 365, 282-290.	2.6	3
203	Applications of reactive molecular dynamics to the study of the thermal decomposition of polymers and nanoscale structures. Materials Science & Engineering A: Structural Materials: Properties, Microstructure and Processing, 2004, 365, 114-121.	2.6	53
204	Effect of carbon on hydrogen desorption and absorption of mechanically milled MgH2. Journal of Power Sources, 2004, 129, 73-80.	4.0	158
205	Metal organic chemical vapour deposition (MOCVD) of bone mineral like carbonated hydroxyapatite coatingsElectronic supplementary information (ESI) available: experimental data. See http://www.rsc.org/suppdata/cc/b3/b312855p/. Chemical Communications, 2004, , 696.	2.2	47
206	Modelling of binder removal from a (fibre+powder) composite pre-form. Acta Materialia, 2003, 51, 899-909.	3.8	9
207	Structural stability of mechanically alloyed (Mg+10Nb) and (MgH2+10Nb) powder mixtures. Journal of Alloys and Compounds, 2003, 349, 217-223.	2.8	56
208	Direct mechanical synthesis and characterisation of Mg2Fe(Cu)H6. Journal of Alloys and Compounds, 2003, 356-357, 626-629.	2.8	20
209	Influence of High Energy Ball Milling on the Carbothermic Reduction of Ilmenite. Materials Science Forum, 2003, 437-438, 105-108.	0.3	7
210	Effects of Additional Rolling and Annealing on the Cube Texture in the High-Purity Aluminum Foils for Capacitors. Materials Science Forum, 2003, 437-438, 455-458.	0.3	0
211	Structural Stability and Dehydrogenation of (MgH ₂ +Al, Nb) Powder Mixtures during Mechanical Alloying. Materials Transactions, 2003, 44, 2356-2362.	0.4	13
212	Influence of interstitial elements on the bulk modulus and theoretical strength of α-titanium: a first-principles study. Philosophical Magazine A: Physics of Condensed Matter, Structure, Defects and Mechanical Properties, 2002, 82, 1345-1359.	0.8	2
213	First Principles Estimation of Bulk Modulus and Theoretical Strength of Titanium Alloys. Materials Transactions, 2002, 43, 3028-3031.	0.4	14
214	Influence of interstitial elements on the bulk modulus and theoretical strength of a-titanium: A first-principles study. Philosophical Magazine A: Physics of Condensed Matter, Structure, Defects and Mechanical Properties, 2002, 82, 1345-1359.	0.8	5
215	First principles studies of TiAl-based alloys. Journal of Light Metals, 2002, 2, 115-123.	0.8	32
216	Microstructure, electrochemical performance and gas-phase hydrogen storage property of Zr0.9Ti0.1[(Ni,V,Mn)0.95Co0.05]α laves phase alloys. Journal of Alloys and Compounds, 2002, 333, 184-189.	2.8	6

#	Article	IF	CITATIONS
217	Comparative study of mechanical alloying of (Mg+Al) and (Mg+Al+Ni) mixtures for hydrogen storage. Journal of Alloys and Compounds, 2002, 336, 222-231.	2.8	63
218	Microstructural modelling of dynamic recrystallisation using an extended cellular automaton approach. Computational Materials Science, 2002, 23, 209-218.	1.4	104
219	First principles study of influence of alloying elements on TiAl: cleavage strength and deformability. Computational Materials Science, 2002, 23, 55-61.	1.4	9
220	Microstructural evolution of a Ti–6Al–4V alloy during thermomechanical processing. Materials Science & Engineering A: Structural Materials: Properties, Microstructure and Processing, 2002, 327, 233-245.	2.6	358
221	Characterisation of structural stability of (Ti(H2)+22Al+23Nb) powder mixtures during mechanical alloying. Materials Science & Engineering A: Structural Materials: Properties, Microstructure and Processing, 2002, 332, 210-222.	2.6	19
222	A diffusion-controlled kinetic model for binder burnout in a powder compact. Acta Materialia, 2002, 50, 1937-1950.	3.8	39
223	A first-principles study of the theoretical strength and bulk modulus of hcp metals. Philosophical Magazine A: Physics of Condensed Matter, Structure, Defects and Mechanical Properties, 2001, 81, 321-330.	0.8	11
224	Cost-Effective Manufacture of Particulate Reinforced Titanium Matrix Composites By A New In-situ Reaction Route. Materials Technology, 2001, 16, 230-233.	1.5	2
225	Reaction synthesis of TiB2–TiC composites with enhanced toughness. Acta Materialia, 2001, 49, 1463-1470.	3.8	190
226	First principles study of site substitution of ternary elements in NiAl. Acta Materialia, 2001, 49, 1647-1654.	3.8	103
227	Coupled quantitative simulation of microstructural evolution and plastic flow during dynamic recrystallization. Acta Materialia, 2001, 49, 3163-3175.	3.8	395
228	A Novel Powder Coated Fibre Pre-processing Route to Metal Matrix Composites. Advanced Engineering Materials, 2001, 3, 223-226.	1.6	7
229	Mechanical Alloying of Fine Structured Ti-Al-Nb Aluminides Involving Ti-Hydride. Materials Science Forum, 2001, 360-362, 421-426.	0.3	0
230	A first-principles study of the theoretical strength and bulk modulus of hcp metals. Philosophical Magazine A: Physics of Condensed Matter, Structure, Defects and Mechanical Properties, 2001, 81, 321-330.	0.8	0
231	Development of a powder coated fibre pre-processing route for production of fibre reinforced composites. Materials Science and Technology, 2000, 16, 862-866.	0.8	6
232	Evidence of the existence an α/β interface phase in a near-α titanium alloy. Materials Science & Engineering A: Structural Materials: Properties, Microstructure and Processing, 2000, 280, 182-186.	2.6	8
233	Co-enhanced SiO2-BN ceramics for high-temperature dielectric applications. Journal of the European Ceramic Society, 2000, 20, 1923-1928.	2.8	151
234	Microstructural characterisation of electroless-nickel coatings on zirconia powder. Scripta Materialia, 2000, 43, 307-311.	2.6	65

#	Article	IF	CITATIONS
235	Processing of in situ toughened b-w-c composites by reaction hot pressing of b4c and wc. Scripta Materialia, 2000, 43, 853-857.	2.6	35
236	Preparation of high porosity metal foams. Metallurgical and Materials Transactions B: Process Metallurgy and Materials Processing Science, 2000, 31, 1345-1352.	1.0	78
237	Novel polymer–metal based method for open cell metal foams production. Materials Science and Technology, 2000, 16, 776-780.	0.8	18
238	Kinetic modelling of binder burnout for optimisation of slurry–powder manufacturing process of Ti/SiC composites. Materials Science and Technology, 2000, 16, 843-847.	0.8	6
239	A first principles study of the influence of alloying elements on TiAl: site preference. Intermetallics, 2000, 8, 563-568.	1.8	75
240	First principles study of influence of alloying elements on TiAl: Lattice distortion. Journal of Materials Research, 1999, 14, 2824-2829.	1.2	9
241	Theoretical study of the effects of alloying elements on the strength and modulus of β-type bio-titanium alloys. Materials Science & Engineering A: Structural Materials: Properties, Microstructure and Processing, 1999, 260, 269-274.	2.6	248
242	Calculation of bulk modulus of titanium alloys by first principles electronic structure theory. Journal of Computer-Aided Materials Design, 1999, 6, 355-362.	0.7	11
243	Microstructure and properties of nippon fire-resistant steels. Journal of Materials Engineering and Performance, 1999, 8, 606-612.	1.2	32
244	Calculation of theoretical strengths and bulk moduli of bcc metals. Physical Review B, 1999, 59, 14220-14225.	1.1	40
245	Viable Routes to Large-scale Commercialisation of Silicon Carbide Fibre Titanium Matrix Composites. Materials Technology, 1999, 14, 133-138.	1.5	8
246	Electroless Plating for the Enhancement of Material Performance. Materials Technology, 1999, 14, 210-217.	1.5	9
247	Stabilisation of TiBx-Coated SiC Fibres by Nitridation. Scripta Materialia, 1998, 38, 1629-1634.	2.6	4
248	Slurry PM: lower cost for high performance MMCs. Metal Powder Report, 1998, 53, 18-21.	0.3	0
249	Towards cost effective manufacturing of Ti/SiC fibre composites and components. Materials Science and Technology, 1998, 14, 864-872.	0.8	17
250	Processing of Ti-SiC metal matrix composites by tape casting. Materials Science and Technology, 1998, 14, 1024-1028.	0.8	5
251	Processing of Ti-SiC metal matrix composites by tape casting. Materials Science and Technology, 1998, 14, 1024-1028.	0.8	10
252	Towards cost effective manufacturing of Ti/SiC fibre composites and components. Materials Science and Technology, 1998, 14, 864-872.	0.8	5

#	Article	IF	CITATIONS
253	The kinetics and mechanism of interfacial reaction in sigma fibre-reinforced Ti MMCs. Composites Part A: Applied Science and Manufacturing, 1997, 28, 131-140.	3.8	135
254	Solid-state fabrication and interfaces of fibre reinforced metal matrix composites. Progress in Materials Science, 1995, 39, 411-495.	16.0	83
255	Theoretical model for solid-state consolidation of long-fibre reinforced metal-matrix composites. Acta Metallurgica Et Materialia, 1994, 42, 461-473.	1.9	17
256	The effect of temporary hydrogenation on the processing and interface of titanium composites. Composites, 1994, 25, 881-886.	0.9	11
257	Interface microstructures in Ti-based composites using TiB2/C-coated and uncoated SiCf after short-term thermal exposure. Composites, 1994, 25, 887-890.	0.9	17
258	Analysis of interfacial defects in solid-state consolidated composites. Composites, 1994, 25, 563-569.	0.9	7
259	Chemistry effects on interface microstructure and reaction in titanium-based composites. Composites, 1994, 25, 630-636.	0.9	11
260	Interfaces in Ti3Al composites reinforced with sigma SiC fibres. Scripta Metallurgica Et Materialia, 1994, 30, 89-94.	1.0	16
261	Fibre uniformity and cavitation during the consolidation of metal-matrix composite via fibre-mat and matrix-foil diffusion bonding. Acta Metallurgica Et Materialia, 1993, 41, 3257-3266.	1.9	12
262	Microstructural characterization in diffusion-bonded SiC/Ti-6Al-4V composites. Journal of Microscopy, 1993, 169, 269-277.	0.8	18
263	Comparison of interfaces in Ti composites reinforced with uncoated and TiB ₂ /Câ€coated SiC fibres. Journal of Microscopy, 1993, 169, 279-287.	0.8	28
264	Processing of titanium matrix composites with hydrogen as a temporary alloying element. Scripta Metallurgica Et Materialia, 1992, 27, 1695-1700.	1.0	16
265	Study of the effect of hydrogen on titanium alloy foils to be used as potential composite matrices. Scripta Metallurgica Et Materialia, 1992, 27, 1021-1026.	1.0	12
266	On the microstructure and thermomechanical processing of titanium alloy IMI685. Materials Science & Engineering A: Structural Materials: Properties, Microstructure and Processing, 1992, 156, 63-76.	2.6	13
267	Effect of stress state on cavitation and hole growth in superplastic AA 7475 aluminium alloy. Materials Science and Technology, 1990, 6, 516-519.	0.8	12
268	Testing models for superplastic bulge forming of domes. Materials Science and Technology, 1990, 6, 510-515.	0.8	17
269	An experimental investigation of the superplastic forming behavior of a commercial al-bronze. Metallurgical and Materials Transactions A - Physical Metallurgy and Materials Science, 1990, 21, 2957-2966.	1.4	2
270	A microanalytical study of the apparent iron content of vanadium carbide precipitates in HSLA steel. Materials Characterization, 1990, 25, 17-36.	1.9	3

#	Article	IF	CITATIONS
271	Modelling of superplastic bulge forming of domes. Materials Science & Engineering A: Structural Materials: Properties, Microstructure and Processing, 1989, 114, 97-104.	2.6	31
272	Modelling of diffusion bonding of metals. Materials Science and Technology, 1987, 3, 945-953.	0.8	72